

UDSpace Institutional Repository
University of Delaware Open Access Articles

Saha, B., Liu, S., Dutta, S., Zheng, W., Gould, N., & Cheng, Z. et al. (2017). Catalytic Hydrodeoxygenation of High Carbon Furylmethanes to Renewable Jet-fuel Ranged Alkanes over a Rhenium Modified Iridium Catalyst. *Chemsuschem*.

DOI: [10.1002/cssc.201700863](https://doi.org/10.1002/cssc.201700863)

© 2017 Wiley-VCH Verlag GmbH & Co. KGaA, Weinheim

This article is made available in accordance with the University of Delaware Faculty Policy on Open Access ([4.2.15](#)) and the publisher's policy.

CHEMISTRY & SUSTAINABILITY

CHEM **SUS** CHEM

ENERGY & MATERIALS

Accepted Article

Title: Catalytic Hydrodeoxygenation of High Carbon Furylmethanes to Renewable Jet-fuel Ranged Alkanes over a Rhenium Modified Iridium Catalyst

Authors: Basudeb Saha, Sibao Liu, Saikat Dutta, Weiqing Zheng, Nicholas S Gould, Ziwei Cheng, Bingjun Xu, and Dionisios G Vlachos

This manuscript has been accepted after peer review and appears as an Accepted Article online prior to editing, proofing, and formal publication of the final Version of Record (VoR). This work is currently citable by using the Digital Object Identifier (DOI) given below. The VoR will be published online in Early View as soon as possible and may be different to this Accepted Article as a result of editing. Readers should obtain the VoR from the journal website shown below when it is published to ensure accuracy of information. The authors are responsible for the content of this Accepted Article.

To be cited as: *ChemSusChem* 10.1002/cssc.201700863

Link to VoR: <http://dx.doi.org/10.1002/cssc.201700863>

WILEY-VCH

www.chemsuschem.org

A Journal of



Catalytic Hydrodeoxygenation of High Carbon Furylmethanes to Renewable Jet-fuel

Ranged Alkanes over a Rhenium Modified Iridium Catalyst

Sibao Liu, Saikat Dutta, Weiqing Zheng, Nicholas S. Gould, Ziwei Cheng, Bingjun Xu, Basudeb Saha*, and Dionisios G. Vlachos*

Catalysis Center for Energy Innovation, Department of Chemical and Biomolecular Engineering,
University of Delaware, Newark, DE 19716, USA

Corresponding authors' emails: vlachos@udel.edu, bsaha@udel.edu

Abstract

Renewable jet-fuel ranged alkanes are synthesized by hydrodeoxygenation of lignocellulose derived high carbon furylmethanes over ReO_x modified Ir/SiO₂ catalysts under mild reaction conditions. Ir-ReO_x/SiO₂ with a Re/Ir molar ratio of 2 exhibits the best performance, achieving a combined alkanes yield of 82-99% from C₁₂-C₁₅ furylmethanes. Catalyst can be regenerated in three consecutive cycles with only ~12% loss in the combined alkanes yield. Mechanistically, the furan moieties of furylmethanes undergo simultaneous ring saturation and ring opening to form a mixture of complex oxygenates consisting of saturated furan rings, mono-keto groups, and mono-hydroxy groups. Then, these oxygenates undergo a cascade of hydrogenolysis reactions to alkanes. The high yield of Ir-ReO_x/SiO₂ arises from a synergy between Ir and ReO_x. The acidic sites of partially reduced ReO_x activate the C-O bonds of the saturated furans and alcoholic groups, while the Ir sites are responsible for hydrogenation with H₂.

Keywords: Furylmethane, iridium, rhenium oxide, hydrodeoxygenation, jet-fuel, branched alkanes

1. Introduction

Due to recent crude oil depletion and global warming concerns, the conversion of biomass into fuels is highly desirable^[1-10]. Production of jet fuel, a mixture of C₈-C₁₆ hydrocarbons, especially from abundant, inexpensive and carbon-neutral lignocellulose, is of significant interest to the International Air Transport Association^[11]. Jet-fuel ranged branched alkanes can be synthesized from cellulose or hemicellulose derived furans (e.g., furfural and 2-methylfuran)^[12-20] in two steps. High carbon furylmethanes with branched chain backbone are first synthesized by C-C coupling of furans with carbonyl functional groups^[19], which are then hydrodeoxygenated (HDO) to alkanes^[5]. C-C coupling reactions over acid or base catalysts have been reported, e.g., hydroxyalkylation/alkylation (HAA)^[12-23], aldol condensation^[24-25], alkylation^[26], benzoic condensation^[27-28], giving high yields^[47]. In contrast, the HDO step is challenging due to the need of high reaction temperatures and H₂ pressure, with concomitant, high energy consumption and undesirable C-C cracking leading to low yield of desired alkanes^[12-18]. Corma et al. conducted HDO of furylmethanes over Pt/C, Pt/C-Al₂O₃, and Pt/C-TiO₂ catalysts in a flow reactor^[13-15]. At 350 °C, these reactions yielded 70-91% jet fuel ranged alkanes. HDO of furylmethanes has also been performed over Ni-W_xC/C, Ni/Hβ, and Ni/HZSM-5 catalysts at high temperatures (>260 °C)^[16-19]. However, high C-C cracking resulted in low selectivity to the desired alkanes, especially when 5,5'-(furan-2-ylmethylene) bis(2-methylfuran)

(trifuran, Scheme 1) and 5,5'-(propane-2,2-diyl)bis(2-methylfuran) (PBM, Scheme 1) were used as oxygenates. Wang et al. also found that a Ni/SiO₂-ZrO₂ catalyst is effective for trifuran HDO at 250 °C, achieving 70% C₁₅ alkanes and 10% methane yields^[20]. In a batch reactor, a Pd/NbOPO₄ catalyst produced about 90% jet-fuel ranged alkanes at 200 °C^[21], however, C-C cracking remained a challenge. Thus, development of efficient catalysts to minimize undesirable C-C cracking is necessary. SiO₂ supported partially reduced rhenium oxide modified iridium catalysts (Ir-ReO_x/SiO₂) are effective for ring opening of cyclic ethers with -OH groups^[29-33], as well as HDO of polyols^[34-37], sugars^[38], hemicellulose^[39], cellulose^[40-41], and angelica lactone dimer^[42] with little C-C cracking. These catalysts are also effective for selective hydrogenation of unsaturated aldehydes to unsaturated alcohols^[43-44]. Spectroscopic characterizations of the catalysts indicate that the Ir metal surface is partially covered with three-dimensional ReO_x clusters^[45]. It was proposed that the Ir-ReO_x/SiO₂ catalyst can heterolytically dissociate H₂ into H⁺ and H⁻ at the interface between the Ir metal and ReO_x species. The dissociated hydrogen species on Ir-ReO_x/SiO₂ is effective for direct, one-step hydrogenolysis of polyols or esters in water. The Ir-ReO_x/SiO₂ catalyst also shows high C-O hydrogenolysis performance in alkane solvent^[46], where a two-step acid-catalyzed dehydration of alcohols and ethers followed by subsequent hydrogenation rather than a direct, one-step hydrogenolysis is preferred. Given the high performance of Ir-ReO_x/SiO₂ catalyst, we hypothesize that it can catalyze HDO of furylmethanes to the corresponding branched chain alkanes with high

carbon efficiency. Branched chain alkanes with 8-16 carbons are ideal, compared to straight-chain alkanes, for jet fuel due to improved cold flow properties.

In this paper, we report for the first time that Ir-ReO_x/SiO₂ is effective for HDO of furylmethanes (Scheme 1) at low temperature (170 °C), achieving high selectivity for desired alkanes. High yields (82 -99%) of jet-fuel ranged alkanes are achieved at a Re to Ir molar ratio of 2 at optimal reaction conditions. A reaction network involving furan ring hydrogenation, ring opening, and C-O hydrogenolysis is also proposed.

2. Experimental

2.1. Catalyst Preparation

Ir-ReO_x/SiO₂ catalysts with varying Re to Ir molar ratios (0~2 with 4 wt% Ir) were prepared by a sequential impregnation method described previously^[34-41]. First, Ir/SiO₂ was prepared by impregnating Ir on SiO₂ (Fuji Silysia G-6, calcined in air at 700 °C for 1 h with a 10 °C /min heating rate, BET surface area 535 m²/g) with an aqueous solution of H₂IrCl₆ (Sigma-Aldrich). After evaporating the solvent at 75 °C and drying at 110 °C for 12 h, the resulting Ir/SiO₂ was impregnated with an aqueous solution of NH₄ReO₄ (Alfa-Aesar). The catalysts were calcined in a crucible in air at 500 °C for 3 h using a 10 °C /min temperature ramp. The same synthetic procedure was followed to prepare other M-ReO_x/SiO₂ catalysts (M=Rh, Ru, Pt and Pd, Re/M=0.5). The metal precursors were RhCl₃ (Alfa-Aesar), RuCl₃ (Strem Chemicals), H₂PtCl₆ (Sigma-Aldrich) and PdCl₂

(Sigma-Aldrich), respectively. The reported metal loadings are based on the theoretical amount of metals used for impregnation. All the catalysts were used in the powder form with a granule size of < 400 mesh.

2.2. Synthesis of Furylmethanes

Four furylmethanes (C₁₂-C₁₅) were synthesized via HAA coupling of 2-methylfuran (2-MF) with carbonyl containing compounds over an improved graphene oxide (IGO) catalyst (Scheme 1) following our previous work^[47]. The coupling reactions were carried out in a round-bottom flask equipped with a reflux condenser and a magnetic stirrer. High yield (85-95%) of furylmethanes was achieved after 6 h under neat conditions and low temperature (60 °C), which was separated by filtration. Furylmethanes in this work include 5,5'-(furan-2-ylmethylene)bis(2-methylfuran) (trifuran), 5,5'-(butane-1,1-diyl)bis(2-methylfuran) (BBM), 5,5'-(propane-2,2-diyl)bis(2-methylfuran) (PBM), and 5,5'-(ethane-1,1-diyl)bis(2-methylfuran) (EBM).

2.3. Activity Tests

HDO of furylmethanes over Ir-ReO_x/SiO₂ catalysts was performed in a 50 mL Parr reactor with an inserted Teflon liner, the catalyst, a magnetic stirrer, and 10 mL solvent (cyclohexane). After sealing the reactor (equipped with a thermocouple, rupture disk, pressure gauge, and gas release valve), the mixture was heated at 200 °C and 5 MPa H₂ for 1 h at 240 rpm for pretreating the catalyst. Upon pretreatment, the reactor was cooled and H₂ was released. Then, furylmethanes (0.3 g) were

added and the reactor was immediately closed. The reactor was purged with H₂ three times (1 MPa), pressurized to 5.0 MPa, and heated to the desired temperature with continuous stirring the reaction mixture at 500 rpm. The heating time to the set temperature was about 25 min. After reaction, the reactor was immediately transferred to an ice bath. The catalyst was separated from the solution by centrifugation. Aside from furylmethanes, experiments with DMF and DMTHF, as model compounds, were conducted. DMF was purified by distillation before use.

High carbon alkane (C₈-C₁₅) products and oxygenated intermediates in the solution were analysed by a gas chromatograph (GC, Agilent 7890A) equipped with an HP-1 column and a flame ionization detector (FID) using icosane (C₂₀) as an internal standard. The injection and FID temperatures were both set at 300 °C. The initial column temperature was held at 40 °C for 5 min, followed by a 10 °C/min ramp to 270 °C, and a 10 min hold at 270 °C. High carbon alkanes and oxygenated intermediates were identified by a GC (Agilent 7890B) mass spectrometer (Agilent 5977A with a triple-axis detector) equipped with a DB-5 column. The injection and FID temperatures were set at 250 °C and 230 °C, respectively. The initial column temperature was held at 40 °C for 4 min, followed by a 10 °C/min ramp to 315 °C, where the temperature was held for 10 min. An HP-INNOWax column was used for analysis of the HDO products of DMF and DMTHF using *n*-nonane as an internal standard. For analysis of DMF/DMTHF HDO products, the GC injector and FID temperatures were both set at 250 °C. The initial column temperature was held at 30 °C for 6

min, followed by a 20 °C/min ramp to 250 °C, where the temperature was held for 1 min. DMF and DMTHF HDO products were identified by a Shimadzu GC-MS-QP2010 with the same column and method. Control experiments showed a small amount of cyclohexane was converted to hexane and low carbon alkanes over Ir-ReO_x/SiO₂. Thus, C₁-C₆ alkanes were not quantified from the HDO of furylmethanes.

The conversion of furylmethanes, DMF and DMTHF and the yield of all products were calculated on carbon basis using the following equations:

$$\text{Conversion [\%]} = \frac{\text{mol of initial reactant} - \text{mol of unreacted reactant}}{\text{mol of initial reactant}} \times 100$$

$$\text{Yield of detected products [\% - C]} = \frac{\text{mol}_{\text{product}} \times \text{C atoms in product}}{\text{mol of total C atoms of initial reactant}} \times 100$$

Spent catalysts were washed with excess methanol, dried in air, and calcined at 500 °C for 3 h before reuse in the next cycle. Control experiments show that a small amount of the solvent, cyclohexane, is converted to *n*-hexane on Ir-ReO_x/SiO₂ under typical reduction and reaction conditions in the HDO of DMF and 2,5-DMTHF. Thus, *n*-hexane is not taken into account in the product distribution in the HDO of DMF and 2,5-DMTHF, which contributes to the relatively low carbon balances in these experiments.

2.4. Catalyst Characterization

X-ray diffraction (XRD) patterns of the reduced and used catalysts were recorded by a diffractometer (Bruker D8) equipped with a Cu K α radiation source ($\lambda=0.154\text{nm}$) at 40 kV and 40

mA. Thermogravimetric analysis of the reduced and recovered catalysts was performed on a TA Q600 HT TGA/DSC. ATR-FTIR spectra (4000-400 cm^{-1}) of the products were recorded on a Thermo Electron Nicolet 8700 FT-IR Spectrometer. XPS experiments were conducted using a Thermo-Fisher K-alpha+X-ray photoelectron spectrometer equipped with a monochromatic aluminum K-alpha X-ray source (400 μm). Before analysis, the Ir-ReO_x/SiO₂ catalyst was reduced in cyclohexane at 200 °C for 1 h following the procedure detailed in activity test section. The sample was further transferred into the K-Alpha⁺ Vacuum Transfer Module (VTM, ThermoScientific) without being exposed to air.

The FTIR spectra of pyridine adsorbed on Ir/SiO₂, ReO_x/SiO₂, and Ir-ReO_x/SiO₂ were collected on an Agilent Cary 660 FTIR Spectrometer equipped with an MCT detector (128 scans at a spectral resolution of 2 cm^{-1}) with a homemade in situ transmission cell. The transmission cell was held at a vacuum level of 0.01 mTorr through a vacuum manifold, which is connected to a mechanical pump and a diffusion pump. A self-standing catalyst wafer was loaded into a custom made sample holder and reduced under a hydrogen stream (20 ml/min) at 200 °C for 1 h. After cooling to room temperature and evacuation, 100 mTorr of pyridine was introduced to the transmission cell via the vacuum manifold, and IR spectra were collected from 50 °C to 150 °C.

3. Results and Discussion

3.1 Optimization of Catalyst Composition

Catalyst activity was assessed with different Re/Ir molar ratios in the range of 0 to 2 (Table 1). The yields of C₈-C₁₅ alkanes are insignificant over the catalysts containing only Ir or ReO_x (Ir/SiO₂ and ReO_x/SiO₂; Entries 1 and 6 of Table 1). Over Ir/SiO₂, the majority of detectable products are oxygenates (47%). ReO_x/SiO₂ results in 45.9% conversion. Coke formation could be the reason for carbon loss over Ir/SiO₂ and ReO_x/SiO₂ catalyzed reactions. In addition, there could be other unidentified oxygenated intermediates. Clearly, single component catalysts are not effective for deoxygenation of the intermediates. In contrast, the yields of C₈-C₁₅ alkanes are high using the Ir-ReO_x/SiO₂ catalysts. As the Re/Ir molar ratio increases, the C₁₅ alkane yield increases due to reduced C-C cracking (Entries 2-5; Table 1). Since a Re/Ir molar ratio of 2 results in optimal selectivity in C₁₅ alkane, it was chosen for subsequent experiments. Similar trend in catalytic activities with varying Re/Ir molar ratios has been reported previously for hydrogenolysis of glycerol^[35], tetrahydrofurfuryl alcohol^[29], and cellulose^[41]. A physical mixture of Ir/SiO₂ and ReO_x/SiO₂ at the same Re/Ir molar ratio as Ir-ReO_x/SiO₂ gives lower yields of alkanes than the Ir-ReO_x/SiO₂ catalyst (Entry 7; Table 1). This indicates a clear synergy between the Ir and the neighboring ReO_x. Other rhenium modified noble metals (M) catalysts: Rh-ReO_x/SiO₂, Ru-ReO_x/SiO₂, Pt-ReO_x/SiO₂ and Pd-ReO_x/SiO₂ with a Re/M ratio of 0.5 were synthesized and evaluated for the HDO of trifuran. Among these, Ru-ReO_x/SiO₂ exhibits the best performance, with a combined C₈-C₁₅ alkanes yield of 36% (Table 1, Entry 8), which is only approximately half of that

for Ir-ReO_x/SiO₂ at the same Re/M value (Table 1, Entry 3). Rh-ReO_x/SiO₂, Pt-ReO_x/SiO₂ and Pd-ReO_x/SiO₂ are ineffective for this reaction, with the combined C₈-C₁₅ alkanes yield below 6%.

This comparison indicates that Ir-ReO_x/SiO₂ is uniquely effective for the HDO of trifuran.

3.2 Time Profile of Reaction, reaction network and proposed reaction mechanism

To understand the reaction network, we investigated the product distribution at various reaction times using the Ir-ReO_x/SiO₂ catalyst with a Re/Ir molar ratio of 2. Figure 1 shows that the complete conversion of trifuran occurs during heating the reaction mixture from room temperature to 180 °C. Almost no alkane was formed and a large amount of oxygenated intermediates mainly with three oxygen atoms were formed. The products at this stage, identified by GC-MS, are C₁₅H₂₈O₃, C₁₅H₂₆O₃, C₁₅H₂₈O₂ and C₁₅H₃₀O and with m/z values of parent ions at 256, 254, 240, and 226, respectively. The main functional groups in these oxygenated intermediates are saturated furan rings, carbonyls, and hydroxyls. Based on the MS and FTIR spectroscopic data (Figure S1), we propose that C₁₅H₂₈O₃ has two saturated rings with one mono-hydroxyl chain (Compounds 1 and 2, Figure 2). The presence of a hydroxyl group is confirmed by the hydroxyl stretching band at 3592-3206 cm⁻¹ observed in ATR-FTIR (Figure S1). Several oxygenates could correspond to an m/z of 254 (C₁₅H₂₆O₃), where all the furan rings of trifuran are fully hydrogenated (Compound 3, Figure 2) or two of them are hydrogenated with one mono-keto chain (Compounds 4 and 5, Figure 2). The presence of a carbonyl group is confirmed by the C=O stretching peak at 1715 cm⁻¹ in ATR-FTIR

(Figure S1). These oxygenates (Compounds 1-5) are the hydrogenated products from trifuran. Intermediate $C_{15}H_{28}O_2$ with an m/z of 240 amu could contain two saturated furan rings with one alkyl branch (Compounds 6 and 7, Figure 2) or one saturated furan ring, with one mono-keto chain and one alkyl branch (Compounds 8 and 9, Figure 2). Compounds 3-5 (Figure 2) are likely formed by deoxygenation of Compounds 1 and 2. There are two intermediates with the parent ion of 226 amu ($C_{15}H_{30}O$), which could be the stereoisomers of the structure with one hydrogenated furan ring and two alkyl branches (Compounds 10, Figure 2). Compound 10 could result from the ring opening of compounds with two saturated furan-rings, e.g., Compound 3, followed by the partial deoxygenation of the two oxygen atoms. As the reaction progresses for 1 h at 180 °C, the amount of oxygenates containing three oxygen atoms decreases with a concomitant increase in the concentration of oxygenates with one or two oxygen atoms. Figure 2 shows that the oxygen content of the oxygenates decreases gradually with time as the amount of C_8 - C_{15} alkanes increases. The oxygenates are fully converted to alkanes within 12 h.

To understand the ring hydrogenation, ring opening and subsequent deoxygenation of trifuran and their oxygenated intermediates, we studied the conversion of DMF and DMTHF as model compounds (Table S1 and S2). In case of DMF conversion, both ring opening products (2-hexanone and 2-hexanol) and ring saturation product (DMTHF) were observed during heating the reaction mixture to 140 °C. The dominant product is DMTHF. In the hydrogenolysis of DMTHF,

almost no conversion of DMTHF was observed during heating to 140 °C, which indicates that the formation of 2-hexanol is proceeded by the hydrogenation of 2-hexanone. Therefore, the ring opening of DMF to 2-hexanone and 2-hexanol and the ring-saturation of DMF to DMTHF occur in parallel over the Ir-ReO_x/SiO₂ catalyst (Scheme S1). This is consistent with the proposed mechanism that hydrogenation of trifuran occurs prior to hydrogenolysis during the heating period. The ring-saturated product (DMTHF) is the dominant product in the conversion of DMF, indicating that the reaction involving trifuran predominantly begins via hydrogenation of unsaturated furan rings. 2-hexanone is quickly hydrogenated to 2-hexanol, which then undergoes hydrogenolysis to *n*-hexane^[48]. The HDO of DMTHF to *n*-hexane likely proceeds through the hydrogenolysis of the C-O ether bond, with 2-hexanol as the intermediate. 2-Hexanone is not detected, which indicates the mono-keto group of oxygenates 4, 5, 8 and 9 (Figure 2) was formed from the direct ring opening of trifuran without prior ring saturation. This finding differs from Corma's work, in which tetrahydrofurans were the intermediates of ketones^[15], likely due to the comparatively low reaction temperature used here. HDO of DMF on Ir-ReO_x/SiO₂ yields primarily ring hydrogenated DMTHF, while ring-opened products, i.e., 2-hexanone and 2-hexanol, are relatively minor (Table S1). This is due to the fact that the formation of DMTHF is more thermodynamically favorable^[49], and thus the ring-opening of DMF occurs via partially and/or fully hydrogenated ring intermediates. This is

consistent with previous work that the ring-opening of DMTHF is more difficult than DMF^[50], and thus requires higher temperatures.

Combining these results, we propose an overall reaction pathway for the HDO of trifuran into jet-fuel ranged alkanes (Scheme 2). In the hydrogenation step (occurred during heating period to the reaction temperature), the furan rings of trifuran underwent ring saturation and ring opening in parallel to form a mixture of complex oxygenates with three different functional branches including saturated furan ring, carbonyl groups and hydroxyl groups. The ring saturation reaction was the main route. Then, carbonyl groups were hydrogenated to the corresponding hydroxyl groups, followed by dehydration and hydrogenation steps to yield alkyl groups. In addition, ring opening, dehydration and hydrogenation of saturated furan rings also led to alkyl branches. Thus, the formation of desired alkanes involved several cascading steps in a complex reaction network over Ir-ReO_x/SiO₂.

To elucidate the relationship between the structure of the catalyst and its performance in the hydrogenolysis of C-O bonds during HDO of trifuran, we characterized Ir-ReO_x/SiO₂ after reduction by XPS (Figure 3), XRD (Figure S2) and FT-IR spectroscopy of pyridine adsorption (Figure 4). XPS was carried out to determine the oxidation states of Ir and Re after the reduction procedure. To avoid air exposure, reduced catalyst sample was transferred in a glove box via Vacuum Transfer Model to the XPS chamber. Both Ir 4f and Re 4f core level spectra of the reduced Ir-ReO_x/SiO₂ are summarized in Figure 3. The Ir 4f spectrum was deconvoluted with Doniach-Šunjić (DS) asymmetric

line shape and Gaussian-Lorentzian sum form (SGL)^[51], which has the binding energies for $4f_{7/2}$ and $4f_{5/2}$ peaks of ~60.8 and 63.8 eV, respectively, indicating that Ir exists in the metallic state. The deconvoluted Re 4f spectrum shows peaks for Re^0 , Re^{2+} and Re^{4+} , which were assigned according to the literature values^[52]. The XPS analysis suggests a significant portion of Re is partially reduced to Re^{2+} and Re^{4+} (41% and 11%, respectively), which is consistent with prior reports of the Ir- $\text{ReO}_x/\text{SiO}_2$ catalyst for the hydrogenolysis of low carbon molecules^[45].

XRD patterns (Figure S2) showed that the peak position of Ir in Ir- $\text{ReO}_x/\text{SiO}_2$ (Re/Ir=2) after reduction was similar to that of Ir/ SiO_2 , which indicated that not an appreciable level of alloying between Ir and Re formed in the Ir- $\text{ReO}_x/\text{SiO}_2$ catalyst, as alloying will change the binding energies of Ir and Re^[53]. In addition, peaks for Re species were not detected at all in the Ir- $\text{ReO}_x/\text{SiO}_2$ (Re/Ir=2) catalyst, suggesting that the Re species are likely highly dispersed.

Transmission FTIR spectroscopy of pyridine adsorbed on the in-situ reduced catalysts (Ir/ SiO_2 , $\text{ReO}_x/\text{SiO}_2$ and Ir- $\text{ReO}_x/\text{SiO}_2$) was used to evaluate their acidic properties. An IR band at 1450 cm^{-1} is assigned to pyridine adsorbed on Lewis acid sites (Figure 3), whereas a band at 1540 cm^{-1} emerges from pyridine interacting with the Brønsted acidic sites. The peak at 1490 cm^{-1} can contain contributions from both Lewis and Brønsted acid sites^[54]. The IR spectrum of pyridine adsorbed on Ir- $\text{ReO}_x/\text{SiO}_2$ (Figure 3) clearly exhibits the presence of Lewis acid sites, which could be due to the partially reduced ReO_x species. A weak but distinctive band at 1540 cm^{-1} was also

observed, indicating the presence of Brønsted acid sites. This is consistent with a prior report, in which Zhang et al. observed both Lewis and Brønsted acid sites on silica supported Ir-ReO_x catalyst after reduction^[33]. In both the Ir/SiO₂ and the ReO_x/SiO₂ catalysts, a significant peak at 1445 cm⁻¹ was observed at 50 °C but pyridine adsorbed on Brønsted acid sites was absent. The peak at 1445 cm⁻¹ could be associated with physically adsorbed pyridine on the silica support^[54]; however, the presence of Lewis acid sites could not be excluded, as the peak at 1445 cm⁻¹ may overlap with the peak at 1450 cm⁻¹. Previously, Davis et al. observed Lewis acid sites on ReO_x supported on silica after reduction in H₂ at 473 K^[52]. When the temperature was increased to 100 °C, surface adsorbed pyridine on Ir/SiO₂ and ReO_x/SiO₂ was fully desorbed. In contrast, Ir-ReO_x/SiO₂ showed peaks corresponding to Brønsted and Lewis acid sites at 150 °C, indicating that an interaction between Ir and ReO_x not only creates Brønsted acid sites absent on individual components, but also enhances the acidic strength of both types of sites. However, we are unable to establish the correspondence between specific oxidation states of Re and acid sites based on the results presented in this work, and thus, no attempt has been made to correlate deconvoluted XPS bands with acid site densities.

The hydrogenolysis of etheric and alcoholic C-O bonds is the final steps in the formation of alkanes over the Ir-ReO_x/SiO₂ catalyst. Tomishige and co-workers have proposed that the hydrogenolysis of secondary mono-alcohols was likely assisted by the Lewis or Brønsted acid sites of Ir-ReO_x/SiO₂^[46], however, they did not characterize acid sites on the catalyst. Dumesic et al.

studied the selective hydrogenolysis of C-O bonds of a wide range cyclic ethers and polyols over a Rh-ReO_x/C catalyst in water solvent^[55-56], and proposed Brønsted acidic sites on ReO_x, associated with metallic Rh, participated in the ring-opening of tetrahydrofuran. Marks et al. reported that high valent metal triflate Lewis acid sites, e.g., Hf(OTf)₄, exhibit high activity in the hydrogenolysis of etheric and alcoholic C-O bonds^[57-58] in an alkane solvent. Taken all together, it is reasonable to infer that the acid sites on the partially reduced ReO_x of the Ir-ReO_x/SiO₂ catalyst could play an important role in activating the C-O bonds of saturated furan ring and promoting the ring-opening to form alcohols as intermediates followed by their dehydration in cyclohexane solvent. Finally, Ir metal catalyzes the hydrogenation of alkenes to produce alkanes.

Two other alkane molecules that form in considerable yields are *n*-decane and *n*-undecane. These may form via C-C bond scission adjacent to the tertiary carbon atom in the middle of trifuran, resulting in the removal of a C₅ or C₄ moiety. Examination of the reaction time profile (Figure 1) reveals that *n*-decane and *n*-undecane formed at the beginning of the reaction. The amount of *n*-decane and *n*-undecane increases only slightly with a proportional decrease in the yield of desired alkane at longer reaction time. This indicates that the fragmentation mainly occurs in the initial stages (Scheme 3), in line with Corma's work^[15], which reported that the C-C bond scission of furylmethane occurs preferentially between a furan moiety and a tertiary carbon atom, catalyzed by acid sites^[15]. Similarly, we observed 2-methyl-5-pentyltetrahydrofuran and

2-hexyl-5-methyltetrahydrofuran intermediates at the beginning of the reaction, which could form via C-C cleavage by surface acid sites on the Ir-ReO_x/SiO₂ catalyst. However, the C-C cleavage of the C₁₅ alkane could not be completely ruled out based on results in this work (Scheme 3).

3.3 Optimizing Reaction Temperature and H₂ Pressure

The effect of the reaction temperature on the HDO of trifuran is shown in Figure 5(a). The yields of C₈-C₁₅ alkanes, with C₁₅ being the major product (41-74%), increase with increasing reaction temperature from 150 °C to 170 °C. Higher temperature (>160 °C) causes a slight decrease in the yield of C₁₅ alkane, owing to forming C-C cleavage products (mainly C₁₀ and C₁₁). The highest yield of C₈-C₁₅ alkanes reaches 91% at 170 °C, with a C₁₅ alkane yield of 75%. Our maximum alkane yield is comparable to a previous report over a Pd/NbOPO₄ catalyst (91%)^[21] and higher than those over Ni/Hβ and Ni/HZSM-5 catalysts (~70%)^[16-18]. Notably, our reaction temperature (170 °C) is lower than previous works (≥200 °C, with several works employing much higher temperatures), underscoring the effectiveness of Ir-ReO_x/SiO₂ for the HDO of trifuran.

It was reported that a two-step reaction with furan ring hydrogenation at low temperature followed by HDO at high temperature was effective for both the conversion of furfural to 1,5-pentendiol over Pd- or Rh-Ir-ReO_x/SiO₂^[30, 31] and the synthesis of hydrocarbons from aldol condensation product of HMF and acetone over a Pd/C-Hf(OTf)₄ catalyst^[59]. To explore the effectiveness of this strategy, we performed a two-step reaction in which the reaction mixture was

heated at 50 °C for 4 h, followed by elevating the reaction temperature to 170 °C to continue the reaction for another 12 h. The yield of C₈-C₁₅ alkanes from the two-step reaction is slightly lower (84%) than that obtained from one-step reaction (91%, Table S3).

The effect of initial hydrogen pressure on the HDO of trifuran is shown in Figure 5(b). The yields of C₈-C₁₅ alkanes increase remarkably as the H₂ pressure increases from 2 to 5 MPa, with C₁₅ exhibiting the highest yield (41-75%). This can be explained by the positive reaction order with respect to H₂ pressure in the HDO over Ir-ReO_x/SiO₂, consistent with prior reports^[29, 35]. Higher H₂ pressure (6 MPa) did not affect the yields of C₈-C₁₅ alkanes. The C-C cracking products (mainly C₁₀ and C₁₁) decrease significantly with increasing H₂ pressure. Since C-C cleavage mainly occurs at the beginning of the reaction, higher H₂ pressure favors hydrogenation and saturation of the furan ring and thus suppresses C-C bond scission in the unsaturated ring trifuran molecule.

3.4 Catalyst Stability

Catalyst reusability is important in determining its potential for practical applications. The results of the reused Ir-ReO_x/SiO₂ (Re/Ir=2) are shown in Table 2. After the 1st cycle, the catalyst is separated from the products by centrifugation, washed with methanol, and dried at 110 °C for 10 h before reuse in the next cycle. Due to a small mass loss of catalyst (7~11 wt%) during recovery, we decreased the scale of each subsequent recycling experiment in which the ratios of catalyst, substrate and solvent were similar to the 1st run. A reduction pretreatment of the catalyst was performed before

every cycle, as discussed in the experimental section. Reusing the catalyst without calcination results in a significant decrease in the yields of C₈-C₁₅ alkanes, with the majority of unconverted intermediates being oxygenates (Entry 2; Table 2). The result of TG-DTA analysis of the recovered catalyst after 1st cycle show ~5 wt% carbon deposition on the catalyst surface (Figure S3) that causes catalyst deactivation. Thus, after drying in air, we calcined the spent catalyst at 500 °C in air for 3 h. After calcination, the recovered catalyst regained comparable activity to that of the fresh catalyst (Entry 3; Table 2). The yields of C₈-C₁₅ alkanes in the 3rd cycle is ~12% lower (80%) than the 1st cycle (91%), suggesting that modest catalyst deactivation does occur. The XRD peaks of the recovered catalyst assigned to the metallic Ir phase became sharper (Figure S4). Calculations using the Scherrer equation indicate an increase of the average crystalline size of Ir particles from 2.5 nm (fresh catalyst) to 3.2 nm after three cycles^[60], consistent with previous reports^[30-31, 39-41]. Therefore, observed activity loss in the 3rd cycle is likely caused by sintering of the catalyst during reaction and regeneration.

3.5 HDO of Other Furylmethanes

Three other furylmethanes of carbon numbers C₁₂-C₁₄ were used for the HDO over the Ir-ReO_x/SiO₂ catalyst at the optimal reaction conditions developed for trifuran (Table 3). GC-MS results show complete conversion of these furylmethanes to alkanes under optimized reaction condition. The yields of the corresponding alkanes with the same number of carbon atoms as the feed

varies between 61 and 96%, while the maximum yield of total jet-fuel ranged alkanes varies between 82 and 99%. C₁₂ furylmethane (EBM) forms C₁₂ alkane with the highest selectivity (99%). The selectivity of other alkanes from their respective furylmethanes decreases in the order of EBM \approx BBM > trifuran > PBM. The results suggest that the Ir-ReO_x/SiO₂ catalyst is effective for the HDO of all furylmethanes used in this work.

The selectivity of alkane products from different furylmethanes can be explained by the relative stability of their respective carbocations. The stability of the carbocations increases in the order of primary < secondary < tertiary < quaternary carbons. The C-C fragmentation at the quaternary carbon adjacent to the furan moiety occurs preferentially. Thus, PBM yields the least amount (61%) of alkanes with its corresponding maximum carbon number (C₁₃) due to the formation of a stable tertiary carbocation by C-C scission. C-C cracking of trifuran, EBM, and BBM involves secondary carbocations which are less stable than the tertiary ones. Trifuran has one additional furan ring compared to EBM and BBM, which can stabilize the adjacent carbocation by conjugation. Therefore, HDO of trifuran yields less alkane of maximum carbon number (C₁₅) than the corresponding alkanes of EBM and BBM.

4. Conclusions

In this work, Ir-ReO_x/SiO₂ catalysts with different Re/Ir molar ratio were used for the production of renewable jet-fuel ranged alkanes (C₈-C₁₅) by HDO of C₁₂-C₁₅ furylmethanes under mild reaction

conditions. High yield (82-99%) of C₈-C₁₅ alkanes is achieved at an optimal Re/Ir molar ratio of 2. The main pathway involves hydrogenation of the furan rings to saturated rings, followed by ring opening to hydroxyl containing chains. A minor parallel pathway involves ring opening of the unsaturated furans to mono-keto and mono-hydroxy units. These parallel pathways lead to the formation of several oxygenated intermediates. Sequential hydrogenolysis of these oxygenates over Ir-ReO_x/SiO₂ forms alkanes via a cascade pathway. Controlled experiments and characterization illustrate a strong synergy between Ir and ReO_x of the catalyst in its high activity for HDO of high carbon furylmethanes. The Ir metal initiates the hydrogenation steps via H₂ dissociation and the acid sites of partially reduced ReO_x activate both etheric and alcoholic C-O bonds.

Acknowledgements

This work was supported as part of the Catalysis Center for Energy Innovation, an Energy Frontier Research Center funded by the U. S. Department of Energy, Office of Science, Office of Basic Energy Sciences under Award Number DE-SC0001004. The authors acknowledge the Advanced Materials Characterization Laboratory at the University of Delaware for providing XRD and TG-DTA facilities and Jeffrey Everhart for helping with GC/GCMS analysis of the reaction products. We also acknowledge instrumentation support for XPS (funded by NSF award number 142149).

References

1. G. W. Huber, S. Iborra, A. Corma, *Chem. Rev.*, **2006**, 106, 4044-4098.
2. J.C. Serrano-Ruiz, R. Luque, A. Sepulveda-Escribano, *Chem. Soc. Rev.*, **2011**, 40, 5266-5281.
3. A. Corma, S. Iborra, A. Velty. *Chem. Rev.*, **2007**, 107, 2411-2502.
4. M. Schlaf, *Dalton Trans.*, **2006**, 4645-4653.
5. Y. Nakagawa, S. Liu, M. Tamura, K. Tomishige, *ChemSusChem*, **2015**, 8, 1114-1132.
6. M. Besson, P. Gallezot, C. Pinel, *Chem. Rev.*, **2014**, 114, 1827-1870.
7. M. J. Climent, A. Corma, S. Iborra, *Green Chem.*, **2014**, 16, 516-547.
8. H. Kobayashi, A. Fukuoka, *Green. Chem.*, **2013**, 15, 1740-1763.
9. Y. Nakagawa, M. Tamura, K. Tomishige, *ACS Catal.*, **2013**, 3, 2655-2668.
10. T. Ennaert, J. V. Aelst, J. Dijkmans, R. D. Clercq, W. Schutyser, M. Dusselier, D. Verboekend, B. F. Sels. *Chem. Soc. Rev.*, **2016**, 45, 584-611.
11. M.-O. P. Fortier, G. W. Roberts, S. M. Stagg-Williams, B. S. M. Sturm, *Appl. Energy*, **2014**, 122, 73-82.
12. A. Bohre, S. Dutta, B. Saha, M. M. Abu-Omar, *ACS Sustainable Chem. Eng.*, **2015**, 3, 1263-1277.
13. A. Corma, O. Torre, M. Renz, N. Vollandier, *Angew. Chem. Int. Ed.*, **2011**, 50, 2375-2378.
14. A. Corma, O. Torre, M. Renz, *ChemSusChem*, **2011**, 4, 1574-1577.

15. A. Corma, O. Torre, M. Renz, *Energy Environ. Sci.*, **2012**, 5, 6328.
16. G. Li, N. Li, J. Yang, L. Li, A. Wang, Y. Cong, T. Zhang, *Green Chem.*, **2014**, 16, 594-599.
17. G. Li, N. Li, J. Yang, L. Li, A. Wang, X. Wang, Y. Cong, T. Zhang, *Bioresour. Technol.*, **2013**, 134, 66-72.
18. S. Li, N. Li, G. Li, L. Li, A. Wang, Y. Cong, X. Wang, G. Xu, T. Zhang, *Appl. Catal. B: Environ.*, **2015**, 170-171, 124-134.
19. S. Li, N. Li, G. Li, L. Li, A. Wang, Y. Cong, X. Wang, T. Zhang, *Green Chem.*, **2015**, 17, 3644-3652.
20. T. Wang, K. Li, Q. Liu, Q. Zhang, S. Qiu, J. Long, L. Chen, L. Ma, Q. Zhang, *Appl. Energy.*, **2014**, 136, 775-780.
21. Q. Xia, Y. Xia, J. Xi, X. Liu, Y. Zhang, Y. Guo, Y. Wang, *ChemSusChem*, DOI: 10.1002/cssc.201601522
22. G. Li, N. Li, S. Li, A. Wang, Y. Cong, X. Wang, T. Zhang, *Chem. Commun.*, **2013**, 49, 5727-5729.
23. G. Li, N. Li, Z. Wang, C. Li, A. Wang, X. Wang, Y. Cong, T. Zhang, *ChemSusChem*, **2012**, 5, 1958-1966.
24. J. Yang, N. Li, S. Li, W. Wang, L. Li, A. Wang, X. Wang, Y. Cong, T. Zhang, *Green Chem.* **2014**, 16, 4879-4884.

25. H. Olcay, A. V. Subrahmanyam, R. Xing, J. Lajoie, J. A. Dumesic, G. W. Huber, *Energy Environ. Sci.*, **2013**, 6, 205-216.
26. K. S. Arias, M. Oteri, A. Corma, H. García, *Energy Environ. Sci.*, **2015**, 8, 317-331.
27. B. L. Wegenhart, L. Yang, S. C. Kwan, R. Harris, H. I. Kenttäm, M. M. Abu-Omar, *ChemSusChem*, **2014**, 7, 2742-2747.
28. L. Wang, E. Y.-X. Chen, *ACS Catal.*, **2015**, 5, 6907-6917.
29. K. Y. Chen, K. Mori, H. Watanabe, Y. Nakagawa, K. Tomishige, *J. Catal.*, **2012**, 294, 171-183.
30. S. Liu, Y. Amada, M. Tamura, Y. Nakagawa, K. Tomishige, *Green Chem.*, **2014**, 16, 617-626.
31. S. Liu, Y. Amada, M. Tamura, Y. Nakagawa, K. Tomishige, *Catal. Sci. Technol.*, **2014**, 4, 2535-2549.
32. Z. Wang, B. Pholjaroen, M. Li, W. Dong, N. Li, A. Wang, X. Wang, Y. Cong, T. Zhang, *J. Energy Chem.*, **2014**, 23, 427-434.
33. B. Xiao, M. Zheng, X. Li, J. Pang, R. Sun, H. Wang, X. Pang, A. Wang, X. Wang, T. Zhang, *Green Chem.*, **2016**, 18, 2175-2184.
34. Y. Nakagawa, Y. Shinmi, S. Koso, K. Tomishige, *J. Catal.*, **2010**, 272, 191-194.
35. Y. Amada, Y. Shinmi, S. Koso, T. Kubota, Y. Nakagawa, K. Tomishige, *Appl. Catal. B: Environ.*, **2011**, 105, 117-127.

36. Y. Amada, H. Watanabe, Y. Hirai, Y. Kajikawa, Y. Nakagawa, K. Tomishige, *ChemSusChem*, **2012**, 5, 1991-1999.
37. Y. Nakagawa, X. Ning, Y. Amada, K. Tomishige, *Appl. Catal. A: Gen.*, **2012**, 433-434, 128-134.
38. K. Y. Chen, M. Tamura, Z. L. Yuan, Y. Nakagawa, K. Tomishige, *ChemSusChem*, **2013**, 6, 613-621.
39. S. Liu, Y. Okuyama, M. Tamuara, Y. Nakagawa, A. Imai, K. Tomishige, *Green Chem.*, **2016**, 18, 165-175.
40. S. Liu, Y. Okuyama, M. Tamuara, Y. Nakagawa, A. Imai, K. Tomishige, *ChemSusChem*, **2015**, 8, 628-635.
41. S. Liu, M. Tamura, Y. Nakagawa, K. Tomishige, *ACS Sustainable Chem. Eng.*, **2014**, 2, 1819-1827.
42. M. Mascal, S. Dutta, I. Gandarias, *Angew. Chem. Int. Ed.*, **2014**, 53, 1854-1857.
43. M. Tamura, K. Tokonami, Y. Nakagawa, K. Tomishige, *Chem. Commun.*, **2013**, 49, 7034-7036.
44. M. Tamura, K. Tokonami, Y. Nakagawa, K. Tomishige, *ACS Catal.*, **2016**, 6, 3600-3609.
45. Y. Aamada, H. Watanabe, M. Tamura, Y. Nakagawa, K. Okumura, K. Tomishige, *J. Phys. Chem. C*, **2012**, 116, 23503-23514.

46. Y. Nakagawa, K. Mori, K. Chen, Y. Aamda, M. Tamura, K. Tomishige, *Appl. Catal. A: Gen.*, **2013**, 468, 418-425.
47. S. Dutta, A. Bohre, G. R. Jenness, W. Zheng, M. Núñez, D. G. Vlachos, B. Saha, *ACS Catal.*, **2017**, 7, 3905–3915.
48. S. Liu, M. Tamura, Y. Nakagawa, K. Tomishige, *Catal. Today*, **2016**, 269, 122-131.
49. M. J. Gilkey, A. V. Mironenko, L. Yang, D. G. Vlachos, B. J. Xu, *ChemSusChem*, **2016**, 9, 3113-3121.
50. G. R. Jenness, W. Wan, J. G. Chen, D. G. Vlachos, *ACS Catal.*, **2016**, 6, 7002-7009.
51. V. Pfeifer, T. E. Jones, J.J. Velasco Vélez, C. Massué, M. T. Greiner, R. Arrigo, D. Arrigo, D. Teschner, F. Girgsdies, M. Scherzer, J. Allan, M. Hashagen, G. Weinberg, S. Piccinin, M. Hävecker, A. Knop-Gericke, R. Schlögl, *Phys. Chem. Chem. Phys.*, **2016**, 18, 2292-2296.
52. D. D. Falcone, J. H. Hack, A. Y. Klyushin, A. Knop-Gericke, R. Schlögl, R. J. Davis, *ACS Catal.*, **2015**, 5, 5679-5695.
53. H. I. Karan, K. Sasaki, K. Kuttiyiel, C. A. Farberow, M. Mavrikakis and R. R. Adzic, *ACS Catal.*, **2012**, 2, 817
54. O. M. Busch, W. Brijoux, S. Thomson, F. Schüth, *J. Catal.*, **2004**, 222, 174-179.
55. M. Chia, Y. J. Pagán-Torres, D. Hibbitts, Q. Tan, H. N. Pham, A. K. Datye, M. Neurock, R. J. Davis, J. A. Dumesic, *J. Am. Chem. Soc.*, **2011**, 133, 12675-12689.

56. M. Chia, B. J. O'Neill, R. Alamillo, P. J. Dietrich, F. H. Ribeiro, J. T. Miller, J. A. Dumesic *J. Catal.*, **2013**, 308, 226-236.
57. Z. Li, R. S. Assary, A. C. Atesin, L. A. Curtiss, T. J. Marks, *J. Am. Chem. Soc.*, **2014**, 136, 104-107.
58. A. C. Atesin, N. A. Ray, P. C. Stair, T. J. Marks, *J. Am. Chem. Soc.*, **2012**, 134, 14682-14685.
59. H. J. Song, J. Deng, M. Cui, X. Li, X. Liu, R. Zhu, W. Wu, Y. Fu, *ChemSusChem*, **2015**, 8, 4250-4255.
60. S. R. Sashital, J. B. Cohen, R. L. Burwell Jr., J. B. Butt, *J. Catal.*, **1977**, 50, 479-493.

Table 1. HDO of trifuran over the Ir-ReO_x/SiO₂ catalyst.

Entry	Catalysts	Re/M molar ratio	Conv. / %	Yield / %									
				C ₈	C ₉	C ₁₀	C ₁₁	C ₁₂	C ₁₃	C ₁₄	C ₁₅	Sum	Oxygenates
1	Ir/SiO ₂	0	98.5	0.0	0.0	0.8	0.9	0.2	0.6		3.3	6	47
2	Ir-ReO _x /SiO ₂	0.25	100	0.0	0.2	9.3	14.0	1.3	0.1		26.6	52	21
3	Ir-ReO _x /SiO ₂	0.5	100	0.0	0.2	9.0	12.7	0.2	0.2		42.3	65	9
4	Ir-ReO _x /SiO ₂	1	100	0.0	0.2	8.6	11.2	0.2	0.3		53.0	75	1
5	Ir-ReO _x /SiO ₂	2	100	0.1	0.2	6.4	7.2	0.3	0.5		60.6	77	0.0
6	ReO _x /SiO ₂	-	45.9	0.0	0.0	0.3	0.3	0.6	0.2		0.4	2	0.0
7 ^a	Ir/SiO ₂ + ReO _x /SiO ₂	-	100	0.0	0.1	7.0	13.4	5.1	0.1		14.2	40	22
8	Ru-ReO _x /SiO ₂	0.5	100	0.5	2.2	8.9	9.9	2.5	1.6		8.3	36	22
9	Rh-ReO _x /SiO ₂	0.5	100	0.0	0.1	0.8	0.8	0.1	0.1		1.1	4	70
10	Pt-ReO _x /SiO ₂	0.5	100	0.0	0.1	1.2	2.1	0.2	0.3		1.4	6	57
11	Pd-ReO _x /SiO ₂	0.5	100	0.0	0.0	0.0	0.0	0.0	0.1		0.1	0.2	52

Reaction condition: catalyst (0.15 g), M: Ir, Rh, Ru, Pt and Pd (4 wt%), trifuran (0.3 g), cyclohexane (10 ml), initial H₂ (5 MPa), 120 h. ^aphysical mixture of Ir/SiO₂ and ReO_x/SiO₂ with the same metal amount of Ir-ReO_x/SiO₂ (Re/Ir=2).

Accepted Manuscript

Table 2. Reusability study of the Ir-ReO_x/SiO₂ (Re/Ir=2) catalyst for the HDO of trifuran.

Entry	Catalyst	Cycle	Conv. / %	Yield / %						C ₁₅	Sum	Oxygenates
				C ₈	C ₉	C ₁₀	C ₁₁	C ₁₂	C ₁₃			
1	Ir-ReO _x /SiO ₂	1	100	0.0	0.1	6.4	8.2	0.3	0.5	74.6	91	0.0
2	Ir-ReO _x /SiO ₂	2 ^a	100	0.1	0.2	9.3	8.4	0.3	0.3	15.9	35	30
3	Ir-ReO _x /SiO ₂	2	100	0.0	0.1	5.6	7.7	0.4	0.5	71.3	87	0.0
4	Ir-ReO _x /SiO ₂	3	100	0.0	0.1	5.5	8.5	0.4	0.4	64.6	80	6.3

Reaction condition: catalyst (0.15 g), Ir (4wt%), trifuran (0.3 g), cyclohexane (10 ml), initial H₂ (5 MPa), 170 °C, 12 h. a: without re-irradiation. Some catalyst mass was lost during recovery. The amounts of fresh or recovered catalysts used in the 1st, 2nd and 3rd cycles were 0.15 g, 0.137 g and 0.128 g, respectively. The weight ratio of catalyst, trifuran and cyclohexane was kept the same in each cycle.

Accepted Manuscript

Table 3. HDO of furylmethanes of carbon numbers 12-15 over the Ir-ReO_x/SiO₂ (Re/Ir=2) catalyst.

Entry	Catalyst	Substrates	Conv. / %	Yield / %						C ₁₅	Sum	Oxygenates
				C ₈	C ₉	C ₁₀	C ₁₁	C ₁₂	C ₁₃			
1	Ir-ReO _x /SiO ₂	Trifuran	100	0.0	0.1	6.4	8.2	0.3	0.5	74.6	91	0.0
2	Ir-ReO _x /SiO ₂	EBM	100	0.0	0.1	0.5	0.6	96.1	0.0	0.8	99	0.0
3	Ir-ReO _x /SiO ₂	BBM	100	0.0	2.4	0.1	0.3	0.4	0.5	1.0	98	0.0
4	Ir-ReO _x /SiO ₂	PBM	100	12.3	0.0	0.3	0.2	2.1	60.8	5.6	82	0.0

Reaction condition: catalyst (0.15 g), Ir (4 wt%), trifuran (0.3 g), cyclohexane (10 ml), initial H₂ (5 MPa), 170 °C, 12 h.

Accepted Manuscript

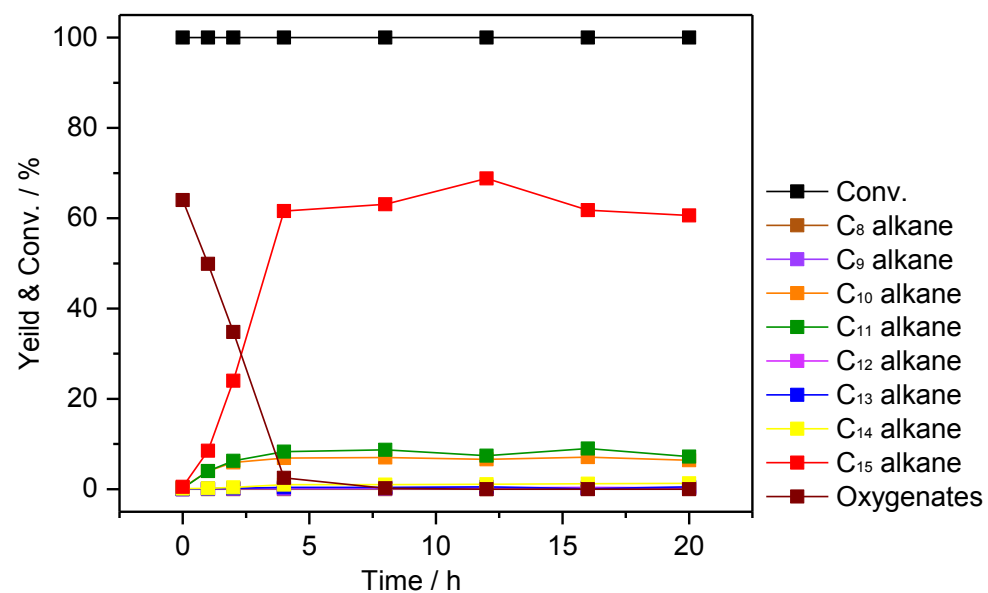


Figure 1. Time dependent results of trifuran HDO over the Ir-ReO_x/SiO₂ (Re/Ir=2) catalyst.

Reaction conditions: catalyst (0.15 g), Ir (4 wt%), trifuran (0.3 g), cyclohexane (10 mL), initial H₂ (5 MPa), 1:

Accepted Manuscript

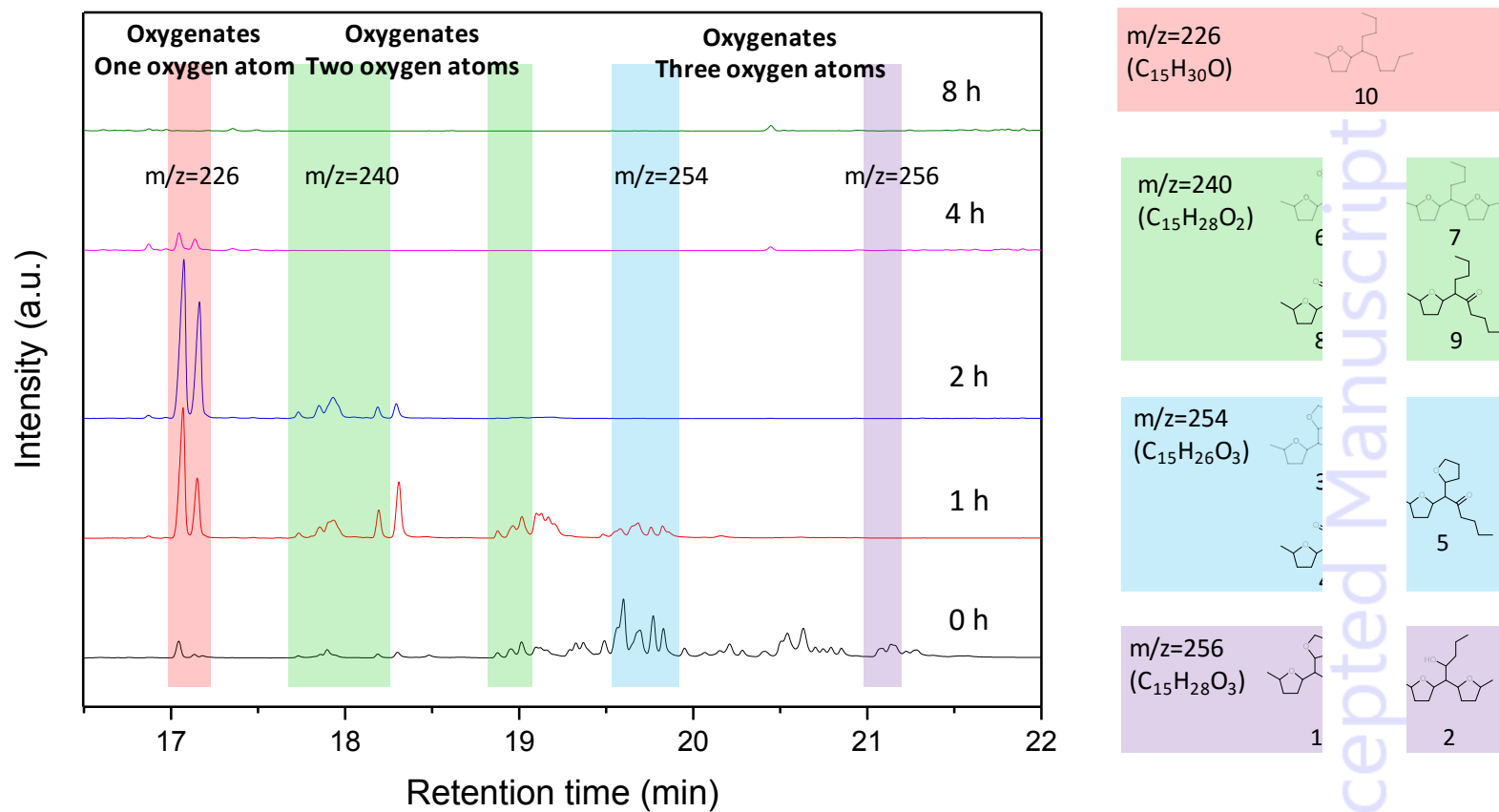


Figure 2. GC chromatograms of the products at different stages of trifuran HDO and possible structures of deoxygenated oxygenates. These oxygenates were identified by GC-MS analysis of the product solutions..

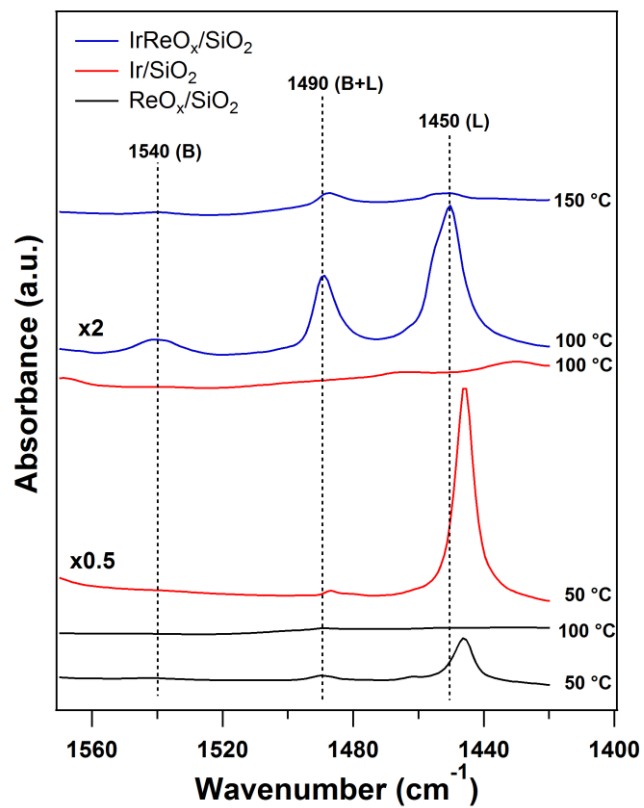


Figure 3. FTIR spectra of adsorbed pyridine on in-situ reduced Ir/SiO₂, ReO_x/SiO₂ and Ir-ReO_x/SiO₂ (Re/ (B): Brønsted acid, (L): Lewis acid.

Accepted Manuscript

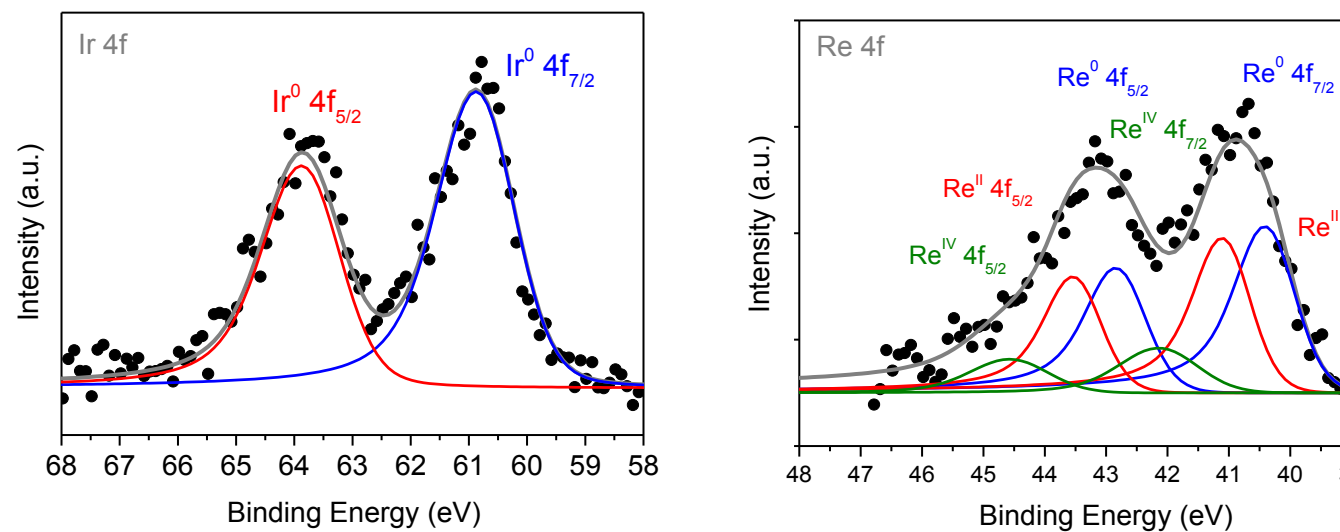


Figure 4. Deconvoluted core-level Ir 4f and Re 4f XPS spectra of Ir-ReO_x/SiO₂ (Re/Ir=2) after reduction.

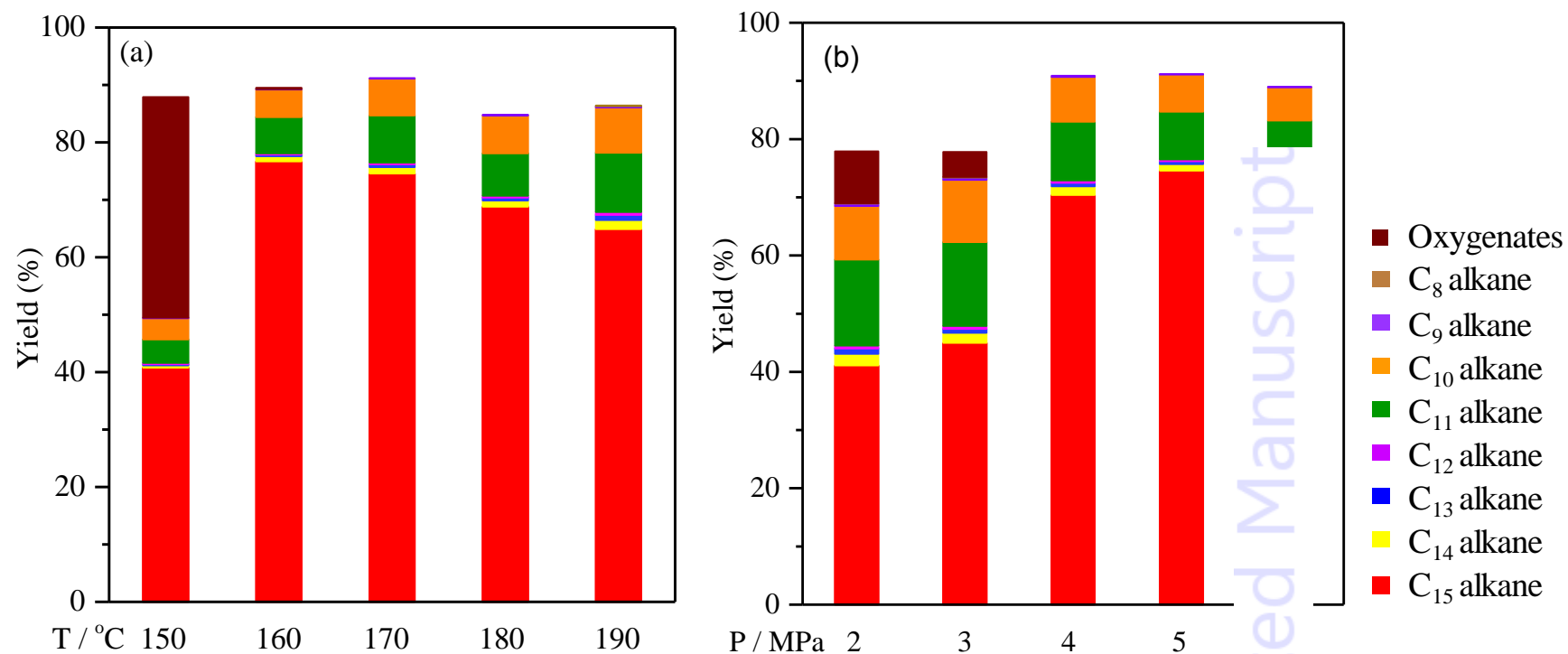
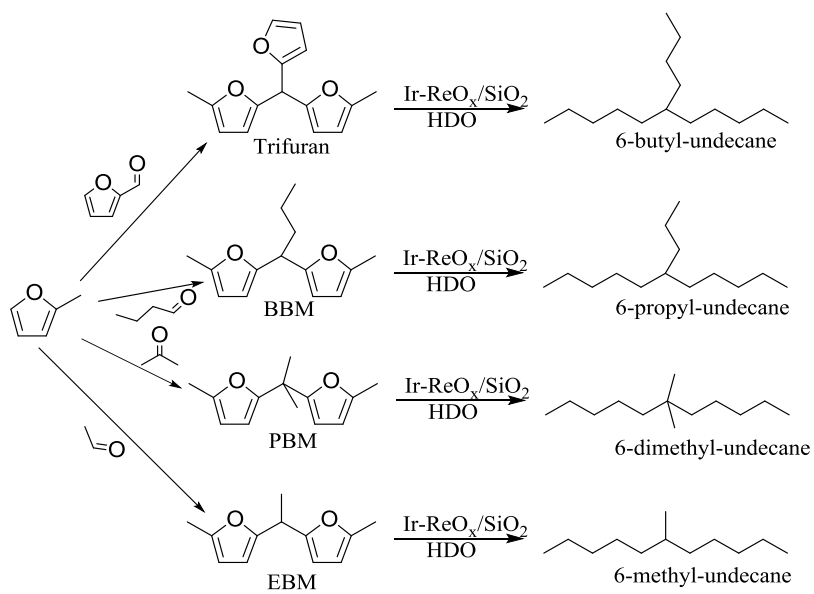
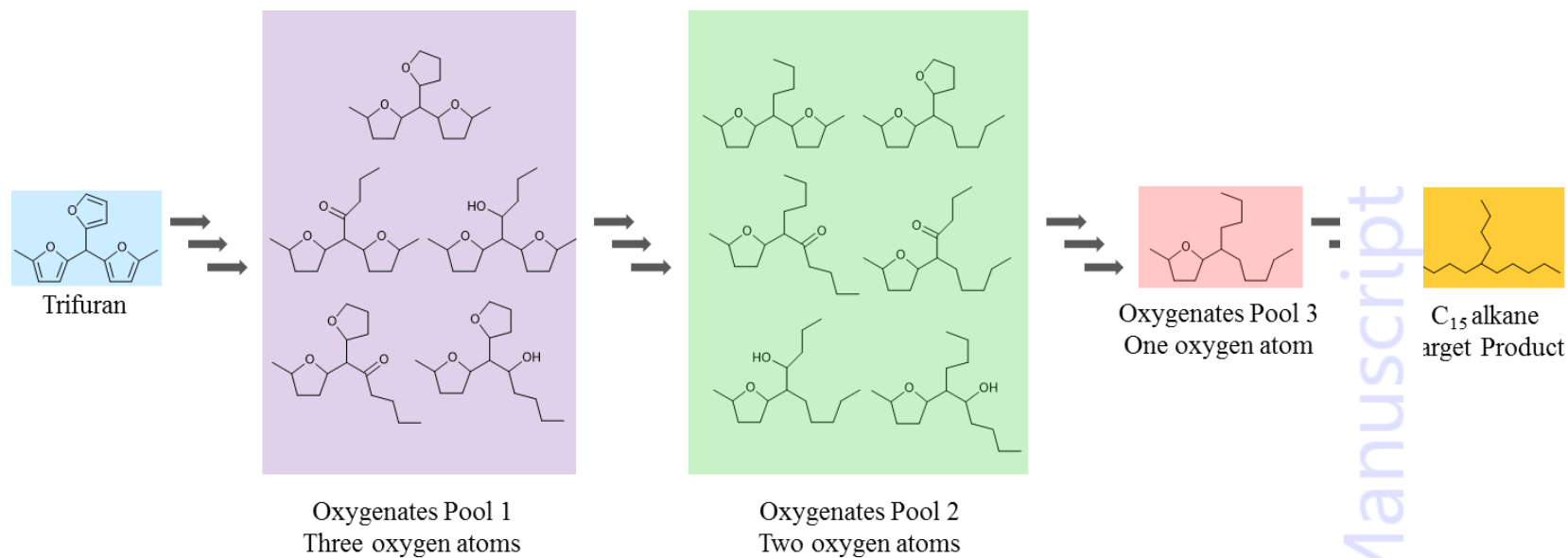


Figure 5. Effects of reaction temperature (a) and hydrogen pressure (b) on the HDO of trifuran over Ir-Re catalyst. Reaction conditions: catalyst (0.15 g), Ir (4 wt%), trifuran (0.3 g), cyclohexane (10 mL), 12 h, (a) initial H₂ (5 MPa), (b) 170 °C.

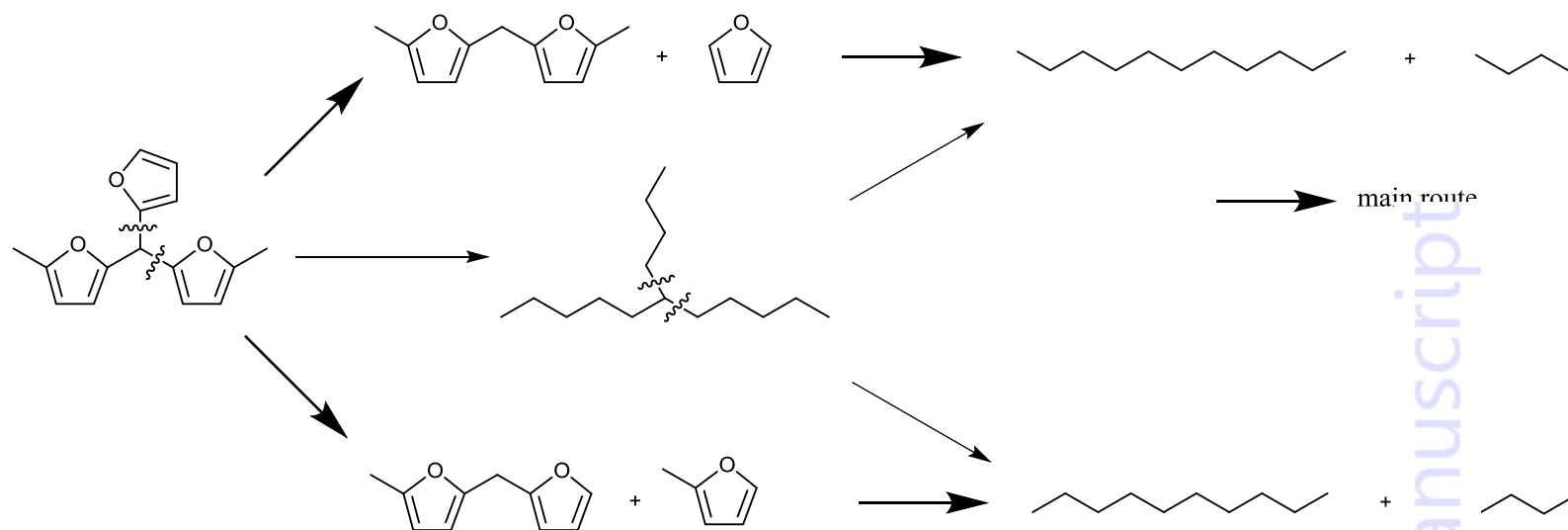


Scheme 1. Synthesis of high carbon oxygenates (trifuran, BBM, PBM, EBM) from low carbon furans using improved graphene oxide catalyst [47] and their subsequent HDO over Ir-ReO_x/SiO₂.

Accepted Manuscript



Scheme 2. Intermediate oxygenates during conversion of trifuran over the Ir-ReO_x/SiO₂ catalyst. These oxygenates were identified from GC-MS analysis of the product solutions.



Scheme 3. Possible pathways for the main C-C cracking product formation during conversion of trifuran.

Accepted Manuscript

Table of contents

High yield of renewable jet-fuel ranged alkanes achieved from high carbon furylmethanes over an Ir-ReO_x/SiO₂ catalyst under mild conditions.

